Segmentation and Simulation of Objects Represented in Images using Physical Principles

Patrícia C.T. Gonçalves[1], João Manuel R.S. Tavares[2] and R.M. Natal Jorge[3]

Abstract The main goals of the present work are to automatically extract the contour of an object and to simulate its deformation using a physical approach. In this work, to segment an object represented in an image, an initial contour is manually defined for it that will then automatically evolve until it reaches the border of the desired object. In this approach, the contour is modelled by a physical formulation using the finite element method, and its temporal evolution to the desired final contour is driven by internal and external forces. The internal forces are defined by the intrinsic characteristics of the material adopted for the physical model and the interrelation between its nodes. The external forces are determined in function of the image features most suitable for the object to be segmented. To build the physical model of the contour used in the segmentation process, the isoparametric finite element proposed by Sclaroff is adopted, and to obtain its evolution towards the object border the methodology presented by Nastar is used, that consists in solving the dynamic equilibrium equation between two consecutive instants.

To simulate the deformation between two different instances of an object, after they each have their contours properly modelled, modal analysis, complemented with global optimization techniques, is employed to establish the correspondence between their nodes (data points). After this matching phase, the displacements field between the two contours is simulated using the dynamic equilibrium equation that balances the internal forces defined by the physical model, and the external forces determined by the distance between the two contours.

keywords: Image analysis, segmentation, deformable models, matching, simulation, finite element method, physical modelling, modal analysis, equilibrium equation.

1 Introduction

In the domain of Computational Vision, namely in image analysis, the identification of an object represented in an image, usually designated by segmentation, is one of the most common and complex tasks. Usually, whenever it is intended to extract higher-level information from an image or even from image sequences, the used image analysis process starts by segmenting the input image(s). Thus, image segmentation is one of the working areas in Computational Vision with more research done and so it will probably continue to be throughout the times.

There are several methods for segmenting objects represented in images; for example, active contours, level set methods, active shape models and deformable templates. Active contours (also known as snakes), introduced by Kass, Witkin and Terzopoulos (1988), use an initial curve that is immersed in a potential field and is elastically deformed by a function of the image features that attracts the curve to the object border. The goal of this method is to minimize the total energy of the curve used in order to define the contour of the object to segment.

With level set methods [Wang, Lim, Khoo and Wang (2007a, b, c), Wang and Wang (2006), Sethian (1999)], the deformation of the contour used in the segmentation task is formulated as a propagating wave front, that is considered as a specific level set of an adopted function. This function has a term of speed defined by the object in the image that stops the propagation of the wave front as soon as it delimits the object. The main idea is to implicitly embed the moving contour into a higher dimensional function and view the contour

[1, 2, 3] Faculdade de Engenharia da Universidade do Porto, Rua Roberto Frias, 4200-465 Porto, Portugal
{patricia.goncalves, tavares, rnatal}@fe.up.pt

[1, 2,] INEGI – Instituto de Engenharia Mecânica e Gestão Industrial

[3] IDMEC – Instituto de Engenharia Mecânica (Pólo FEUP)

as its zero level set [Ma, Tavares and Jorge (2008)].

Active shape models [Vasconcelos and Tavares (2006)] need *a priori* knowledge of the object: the object to segment is sampled by a set of keypoints in each of the images of a training set, as well as by the gray levels around each point. Then, the several sets of keypoints of the training images are aligned to minimize the distance between corresponding points and, analyzing the variation of that distance, the point distribution model is built and used to define an average shape for the object in question and to restrict its deformation during the segmentation process of that object in new images.

Another method that also uses *a priori* knowledge on the object to segment is the one based on deformable templates [Carvalho and Tavares (2006)]. The geometrical templates used are defined by parameters, which describe the expected geometrical shape of the object involved, and interact dynamically with the image data during the segmentation process. As with snakes, an energy function is defined that attracts the template to the object border, the minimum of this energy corresponding to the best possible segmentation that can be accomplished.

As for simulation, the idea of considering physical constraints in object modelling has been suggested and used in Computational Vision by several authors. Terzopoulos, Platt, Barr and Fleischer (1987), for example, employed the elasticity theory to model the behaviour of non-rigid curves, surfaces and solids. These elastically deformable models respond to external forces and interact with neighbour objects. The dynamic equilibrium equation, also known as equation of motion, governs the dynamics of the deformable model under the influence of applied forces.

Terzopoulos, Witkin and Kass (1988) proposed a physically based model for shape and motion reconstruction of deformable objects from images. In that work, the objects were modelled as elastically deformable bodies subjected to mechanical laws.

Sclaroff and Pentland (1995) used the modal matching method to establish correspondences between objects physically modelled, and modal strain energy for object recognition – the lower the energy resulting from deforming a given object into another, the higher the similarity between them.

Using the finite elements method together with modal analysis, Pentland and Horowitz (1991) simulated the physics of elastic non-rigid motion obtaining good estimates for object shape and velocity.

Pinho and Tavares (2004a) used the equation of motion to obtain 2D and 3D dynamic pedobarography transitional objects from two given images.

These and other works have proven that when objects are represented according to physical principals the deformation, namely its non-rigid component, can be adequately modelled.

One of the main goals of this work is to simulate the movement and/or deformation of an object using two images of that object in different instants. For that, one starts by segmenting the object in the two images by extracting its contour. To do so, an initial contour needs to be manually defined, that will evolve throughout an iterative process until it reaches the border of the object. For that purpose, a deformable model is built for the contour using the finite elements method, namely Sclaroff's (1995) isoparametric finite element, and its behaviour towards the object's border is modelled by the dynamic equilibrium equation, thus making it accordingly to physical principles, as proposed by Nastar (1994).

To simulate the deformation between the two contours, Shapiro and Brady (1992) modal shape description is considered, complemented with the optimization search techniques proposed by Bastos and Tavares (2006) to match the nodes of the physical model of one contour to the other. Then, the deformations field is estimated using the approach proposed by Terzopoulos, Platt, Barr and Fleischer (1987) and Terzopoulos, Witkin and Kass (1988) to do realistic deformation simulations considering an elastic model based on the resolution of the dynamic equilibrium equation.

In this paper, a solution to apply this physical approach to contours that do not have all nodes successfully matched is proposed – a common situation when complex objects or large non-rigid deformations are involved.

The herein used methodology is briefly described in Fig. 1. The first step consists in drawing a rough contour on each of the two input images that is considered as the initial segmentation contour for the object. Next, each contour is modelled according to physical principles using the isoparametric finite element proposed by Sclaroff. To move the physical model towards the border of the object in each input image, the dynamic equilibrium equation is solved describing the equilibrium between the internal and external forces considered. The internal forces are defined by the physical characteristics adopted for the model, determined by the adopted virtual material and the selected level of interaction between the nodes of the model; and the external forces are computed by enhancing particular features of the object in the input image. In this work, we consider external forces based on intensity, edges and the distance from each pixel to its nearest edge. After the extraction of the two contours, the nodes of their physical models are matched and the deformation of one into the other is simulated by solving the dynamic equilibrium equation, considering now the external forces as a function of the distance between the two contours.

The main contributions presented in this work are the following: the adoption of the finite elements method to physically model the considered objects, instead of the usual method of the finite differences; the adaptive solution to determine de external forces applied to the model nodes on the segmentation task; and the solution to compute the external forces involved in the simulation when the nodes of the model are not successfully matched.

This paper is organized as follows: section 2 describes how the physical models are built; the next section explains how

objects nodes may be matched using the modal approach complemented with an optimization search algorithm; section 4 refers to the equations that govern the segmentation and simulation tasks; in section 5 some experimental results are presented and analysed; and finally, section 6 concludes the paper and presents some perspectives of future work.

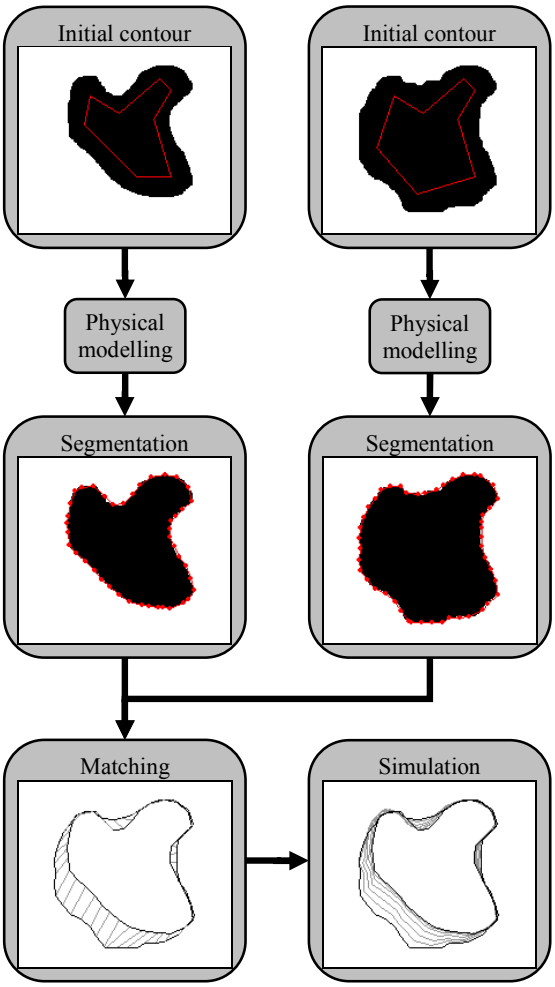

Figure 1: Schema of the methodology used in this work to segment, match and simulate objects represented in images.

2 Physical Modelling

After defining the initial contour for the object to segment, it is time to computationally model it in physical terms; that is, to assign mass, stiffness and damp to each point of the contour, i.e., to each node of the used model.

To model the initial contour and simulate its elastic behaviour, Nastar (1994) used affine interpolation functions together with finite differences. Instead, Gaussian interpolants and the finite element method are used in this work for the same purpose. Namely, the isoparametric finite element proposed by Sclaroff (1995) is considered to build the physical model. This finite element uses a set of radial base functions that allows an easy insertion of the data points in the model. Therefore, Gaussian interpolants are used and the nodes of the model do not need to be previously ordered. Adopting this isoparametric finite element, when an object is modelled it is as if each of its feature points are covered by an elastic membrane [Tavares, Barbosa and Padilha (2000), Sclaroff and Pentland (1995)].

Thus, starting with a collection of m sample points $\mathbf{X}_i(x_i,y_i,z_i)$ of the object to be physically modelled, the interpolation matrix $\mathbf{H}$, which relates the distances between the object nodes and their interrelations, of Sclaroff's isoparametric finite element [Sclaroff (1995), Sclaroff and Pentland (1995)] is built using:

$$g_i(\mathbf{X}) = e^{-\|\mathbf{X}-\mathbf{X}_i\|^2/2\sigma^2}, \tag{1}$$

where σ is the standard deviation that controls the nodes interaction. As Shapiro and Brady (1992) put it, it is "like placing a small circle around a feature (…) and only allowing it to interact with those features (…) lying within the circumference" with radius σ.

Then, the interpolation functions, h_i, are given by:

$$h_i(\mathbf{X}) = \sum_{k=1}^{m} a_{ik} g_k(\mathbf{X}), \tag{2}$$

where a_{ik} are coefficients that satisfy $h_i = 1$ at node i and $h_i = 0$ at the other m-1 nodes. These interpolation coefficients compose matrix $\mathbf{A}$ and can be determined by inverting matrix $\mathbf{G}$ defined as:

$$\mathbf{G} = \begin{bmatrix} g_1(\mathbf{X}_1) & \cdots & g_1(\mathbf{X}_m) \\ \vdots & \ddots & \vdots \\ g_m(\mathbf{X}_1) & \cdots & g_m(\mathbf{X}_m) \end{bmatrix}. \tag{3}$$

Thus, matrix $\mathbf{H}$ will be:

$$\mathbf{H} = \begin{bmatrix} h_1 & \cdots & h_m & 0 & \cdots & 0 \\ 0 & \cdots & 0 & h_1 & \cdots & h_m \end{bmatrix}, \tag{4}$$

and the mass matrix of Sclaroff's isoparametric element is defined as [Sclaroff (1995), Sclaroff and Pentland (1995)]:

$$\mathbf{M} = \begin{bmatrix} \mathbf{M}' & 0 \\ 0 & \mathbf{M}' \end{bmatrix}, \tag{5}$$

where $\mathbf{M}'$ is a sub-matrix $m \times m$ defined as $\mathbf{M}' = \rho\pi\sigma^2\mathbf{A}^{\mathrm{T}}\mathbf{\Gamma}\mathbf{A} = \rho\pi\sigma^2\mathbf{G}^{-1}\mathbf{\Gamma}\mathbf{G}^{-1}$, as matrix $\mathbf{A}$ is symmetric $\mathbf{A}^{\mathrm{T}} = \mathbf{A}$, ρ is the mass density, and the elements of matrix $\mathbf{\Gamma}$ are the square roots of the elements of matrix $\mathbf{G}$.

On the other hand, the stiffness matrix is given by:

$$\mathbf{K} = \begin{bmatrix} \mathbf{K}_{11} & \mathbf{K}_{12} \\ \mathbf{K}_{21} & \mathbf{K}_{22} \end{bmatrix}, \tag{6}$$

where $\mathbf{K}_{ij}$ are symmetric $m \times m$ sub-matrices depending on the constants α, β and λ that are functions of the virtual material adopted for the object [Sclaroff (1995), Sclaroff and Pentland (1995)] defined as:

$$K_{11_{ij}} = \pi\beta \sum_{k,l} a_{ik} a_{jl} \left[\frac{1+\lambda}{2} - \frac{\hat{x}_{kl}^2 + \lambda\, \hat{y}_{kl}^2}{4\sigma^2} \right] \sqrt{g_{kl}} \,, \tag{7}$$

$$K_{22_{ij}} = \pi\beta \sum_{k,l} a_{ik} a_{jl} \left[\frac{1+\lambda}{2} - \frac{\hat{y}_{kl}^2 + \lambda\, \hat{x}_{kl}^2}{4\sigma^2} \right] \sqrt{g_{kl}} \,, \tag{8}$$

$$K_{12_{ij}} = K_{21_{ij}} = -\frac{\pi\beta(\alpha+\lambda)}{4\sigma^2} \sum_{k,l} a_{ik} a_{jl} \hat{x}_{kl} \hat{y}_{kl} \sqrt{g_{kl}} \,, \tag{9}$$

where $\hat{x}_{kl} = x_k - x_l$, $\hat{y}_{kl} = y_k - y_l$, $\hat{z}_{kl} = z_k - z_l$.

In this work, as proposed, for example, by Pinho and Tavares (2004b), Rayleigh's damping matrix, **C**, is used which is a linear combination of the mass and stiffness matrices with constraints, μ and γ, based upon the chosen critical damping [Bathe (1996), Cook, Malkus and Plesha (1989)]:

$$\mathbf{C} = \mu\mathbf{M} + \gamma\mathbf{K} \,. \tag{10}$$

3 Matching the Objects Nodes

After having extracted the contours of the two instances of the desired object, called initial and target objects from here on, it is necessary to find the correspondences between their nodes. For that, a generalized eigenvalue/eigenvector problem is solved for each object using:

$$\mathbf{K\Phi} = \mathbf{M\Phi\Omega} \,, \tag{11}$$

where $\mathbf{\Phi}$ is the modal matrix of the shape vectors (eigenvectors) which describe the modal displacement (u,v) of each node due to vibration mode i, and $\mathbf{\Omega}$ is the diagonal matrix whose entries are the squared eigenvalues increasingly ordered.

After building the modal matrix for each object, the nodes of the two objects can be matched comparing their displacements in the respective modal eigenspace [Shapiro and Brady (1992)]. The main idea of modal matching is that low order modes of two similar shapes will be very close even in the presence of affine transformation, non-rigid deformations, local shape variations or noise. Thus, to match the nodes of the initial object, I, with the ones of the target object, T, an affinity matrix, **Z**, is built with elements defined as:

$$Z_{ij} = \left\| u_{I,i} - u_{T,j} \right\|^2 + \left\| v_{I,i} - v_{T,j} \right\|^2 , \tag{12}$$

where the affinity between nodes i and j is 0 (zero) if the match is perfect, and increases as the match worsens.

In this work, two search methods are considered to find the best matches: a local method and a global one. The local search method was proposed by Shapiro and Brady (1992), and consists in searching each row and each column of the affinity matrix for their lowest values. If the lowest value of row i is in column j, and that value is also the lowest of its column, then node i of the initial object matches node j of the target one. This procedure has the main disadvantage of disregarding the objects structure as it searches for the best match for each node [Bastos and Tavares (2006)].

On the other hand, the global search method proposed by Bastos and Tavares (2006) consists in describing the matching problem as an assignment problem, and solving it using an appropriate optimization algorithm. In this matching approach, cases in which the number of nodes in the initial and target objects is different can also be considered: initially the global matching algorithm adds fictitious nodes to the object with fewer ones, and then the nodes that are matched with the fictitious elements are adequately matched with real nodes using neighbourhood and affinity criteria. Based on this work, a new optimization approach using dynamic programming was proposed by Oliveira and Tavares (2008) to solve the same global matching problem, obtaining better results and in less time.

4 Equilibrium Equation

After having the initial contour transformed into an elastic physical model it is necessary to estimate its evolution in the direction of the object edges to achieve the desired segmentation; and after having both contours extracted from the initial and target objects it is necessary to simulate the deformation of one into the other. To achieve both of these goals, the second order ordinary differential equation, commonly known as Lagrange's dynamic equilibrium equation, is solved:

$$\mathbf{M\ddot{U}}^t + \mathbf{C\dot{U}}^t + \mathbf{KU}^t = \mathbf{F}^t \,, \tag{13}$$

for each time step t, where $\mathbf{U}$, $\dot{\mathbf{U}}$ and $\ddot{\mathbf{U}}$ are, respectively, the displacement, velocity and acceleration vectors, and **F** represents the external forces [Gonçalves, Pinho and Tavares (2006), Pinho and Tavares (2004a)]. This equation describes the equilibrium between the internal and external forces involved on the model nodes. The internal forces are defined by the physical characteristics of the model, determined by the adopted virtual material and the level chosen for the interaction between the nodes of the model, which is considered while building Sclaroff's isoparametric finite element. The external forces depend on whether one is dealing with the segmentation or the simulation of objects deformation, as explained in the following sections.

4.1 External Forces for the Segmentation

To segment an object, the external forces, **F**, are determined by the image features that best describe the object to segment. In particular, the intensity value of each pixel of the initial image, the value of the pixels of the edges image, and

the distance from each pixel to the nearest edge. Thus, $\mathbf{F}$ is the sum of the forces due to the edges image, $\mathbf{F}_{edg}$, the intensity original image, $\mathbf{F}_{int}$, and the distance image, $\mathbf{F}_{dist}$:

$$\mathbf{F} = \mathbf{F}_{edg} + \mathbf{F}_{int} + \mathbf{F}_{dist}. \quad (14)$$

Here, the edges image is obtained by applying Shen and Castan's (1992) edge detection operator to the original image, and the distance image is obtained by calculating the distance of each pixel to its nearest edge using the chamfering algorithm [Sonka, Hlavac and Boyle (2008)].

After the physical modelling of the initial contour defined by the user in the input image, the algorithm calculates the line orthogonal to the tangent at each node of the model. It is along each one of these orthogonal lines that the external forces are calculated. Denoting as Q_i all the pixels belonging to the orthogonal line of node P, the edges force at point P is given by:

$$\mathbf{F}_{edg}(P) = r\frac{\sum_{i=1}^{N} Edg(Q_i)}{N}, \quad (15)$$

where $Edg(Q_i)$ is the value of the pixel Q_i in the edges image, r is a stiffness constant and N is the number of pixels of the orthogonal line. The intensity and distance forces are analogously defined.

If $\|\mathbf{F}(P)\|$ is less than a given threshold then the length of P's orthogonal line will continually grow until $\|\mathbf{F}(P)\|$ reaches that threshold. Thus, each line has the necessary length to determine a sufficient force to move its associated node.

To determine the direction of the external forces, one considers that the pixels of line L (the orthogonal line at node P) to the right of the vertical line that intersects node P have negative values and the ones to the left have positive values, as can be seen in Fig. 2. Thus, if, for example, the sum of the negative values in the edges image is higher than the sum of the positive ones, then the direction of $\mathbf{F}_{edg}$ will be "down", in the case illustrated in Fig. 3. If line L happens to coincide with the vertical line, then the values of the pixels below node P are considered negative.

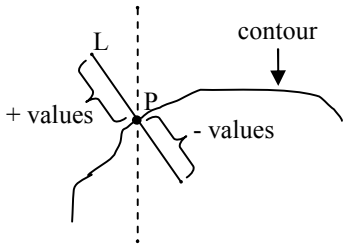

Figure 2: The pixels of line L to the right of the vertical line that passes through node P of the contour have negative values and the ones to the left have positive ones.

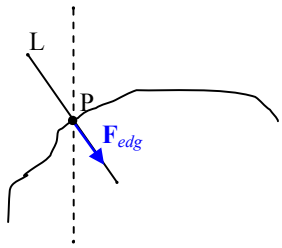

Figure 3: The direction of $\mathbf{F}_{edg}$ if the sum of the positive pixels values in the edges image is higher than the sum of the negative ones.

4.2 External Forces for the Simulation

In the simulation task, to estimate the external force applied on each matched node i of the initial object, we consider that the force on each node is proportional to its associated displacement [Pinho and Tavares (2004b)]:

$$\mathbf{F}(i) = q\left(\mathbf{X}_{T,i} - \mathbf{X}_{I,i}\right), \quad (16)$$

where $\mathbf{F}(i)$ is the force applied on node i, $\mathbf{X}_{I,i}$ the coordinates of node i in the initial object, $\mathbf{X}_{T,i}$ the coordinates of the node corresponding to node i in the target object and q is a global stiffness constant. Because this equation is updated after each iteration of the resolution of the dynamic equilibrium equation, its generalized form is:

$$\mathbf{F}(i) = q\left(\mathbf{X}_{T,i} - \mathbf{X}_{J,i}\right), \quad (17)$$

where $\mathbf{X}_{J,i}$ represents the coordinates of node i in the shape obtained in the J^{th} iteration.

However, some nodes of the initial object may not be successfully matched with any of the nodes in the target object. To overcome this problem, suppose that b is an unmatched node between nodes a and c, matched with nodes a' and c' of the target object, respectively (Fig. 4). Therefore, if b is the i^{th} node in the J^{th} shape, then the i^{th} component of the external force vector is considered as:

$$\mathbf{F}(i) = q\left(\sum_{p\ (\text{nodes between } a' \text{ and } c')} \left[W_p\left(\mathbf{X}_{F,p} - \mathbf{X}_{J,b}\right)\right]\right), \quad (18)$$

where W_p is the weight of node p, according to its matching affinity with node b provided by Eq. 12 – thus, the higher the matching affinity value, the lower the weight.

If there are no unmatched nodes between nodes a' and c', then a' and c' will be considered in the computation of the external force on node b.

5 Some Results

To illustrate the experimental results of the methodology here proposed to segment an object represented in an image by

identifying its contour, consider the images in Fig. 5. In the first one it is possible to see, in red, the initial contour manually defined for the object. The second image represents the segmentation obtained using a physical model with 122 nodes (points) and made of rubber, and considering r=2,000N/m. In this case, the computational process took 15s to achieve the final result. (In this work a personal computer with an Intel Pentium D at 3GHz processor and 2GB of RAM was used, running with Microsoft Windows XP.)

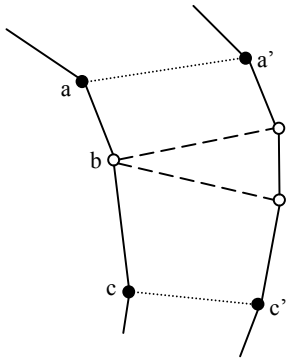

Figure 4: Estimation of the external forces applied on unmatched nodes.

Figure 5: Initial contour (top); result of the segmentation process using r=2,000N/m and considering a rubber model (bottom).

If the same initial contour is modelled with copper instead of rubber, using r=7,000N/m would make the segmentation process take over four hours to finish. Because copper is more rigid than rubber it can support bigger external forces, so if r takes bigger values the process continues to run without numerically diverging. In fact, using r=1x10^{6}N/m in the 122 nodes model made of copper, the segmentation is achieved after 11.5 minutes. Even with a much higher r the segmentation process using a copper model takes a lot longer to finish than using rubber as the adopted virtual material, which is consistent with the expected behaviour of real objects, because it is easier and faster to deform objects made of rubber than of copper.

The initial contour in Fig. 5 was drawn close to the object to segment, but with our methodology, because of the adaptive approach considered for the external forces, that has not be so. The initial contour can be drawn further away from the object border, but that slows down the segmentation process because each pixel has a longer path to go through. The example in Fig. 6 uses the same object and the same initial parameters to build the physical model as the one in Fig. 5, but uses an initial contour defined further away from the object to segment. In this case, the segmentation process takes 100s to finish.

Figure 6: Initial contour defined further away from the object (top); result of the segmentation process using r=2,000N/m and a rubber model (bottom).

In the case of more complex segmentation cases, such as when the objects are partially overlapped, like the ones in Fig. 7, the final result may not be the expected one, because features belonging to other objects can be stronger than the ones of the object to segment, consequentially attracting some nodes of the model to the wrong object.

The segmentation of the hand in Fig. 8 was obtained in 18s, using a physical model with 67 nodes and made of rubber, and considering r=2,000N/m. Fig. 9 shows the same hand but in a different configuration; its physical model had 66 nodes, r=2,000N/m, and was also made of rubber. Its segmentation took 18s.

Using the global search method mentioned before in section 3 to determine the correspondences between the nodes of the contours shown in Figs. 8 and 9, all the 67 nodes of the initial object are successfully matched to the 66 of the target object (Fig. 10). Using q=30,000N/m to calculate the external

forces, the intermediate shapes in Fig. 10 are estimated with Eq. 13 after 100s.

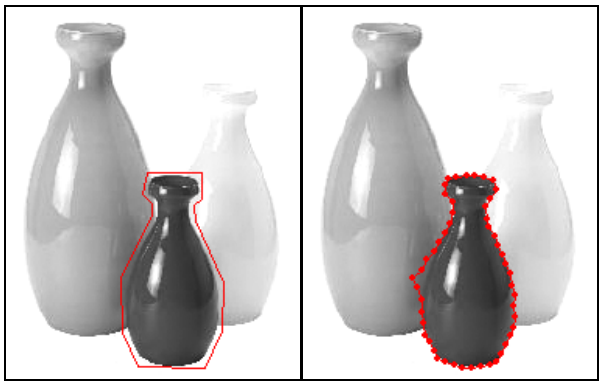

Figure 7: Initial contour (left); result of the segmentation with r=2,000N/m considering a model with 50 nodes and made of rubber (right).

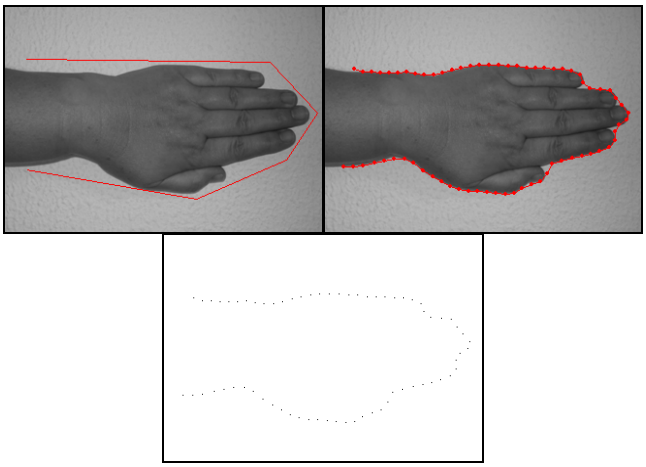

Figure 8: Initial contour (top left); result of the segmentation with r=2,000N/m considering a model with 67 nodes and made of rubber (top right); nodes of the contour extracted (bottom).

The local search method only matches 54 of the 67 nodes of the model of the initial contour; however, with q=30,000N/m and employing Eq. 18 instead of Eq. 17 to determine the external force applied to each unmatched node, the simulation of the deformation between the two instances of the hand is identical to the one with all the nodes matched (Fig. 11), but it takes 210s to finish. This behaviour shows that the present approach to compute the external forces applied to the unmatched nodes seems to be adequate and valid as the results are very similar to the ones obtained with all the nodes successfully matched.

6 Conclusions and Future Work

The experimental results obtained using the physically driven segmentation methodology presented in this paper are quite satisfactory and according to the physical behaviour expected for real objects. However, this approach still presents two drawbacks:

- it becomes slower if the initial contour is not close to the object to be segmented;
- the segmentation result can be compromised when the image in which the object is represented is complex, with noisy data or objects overlapped, for example.

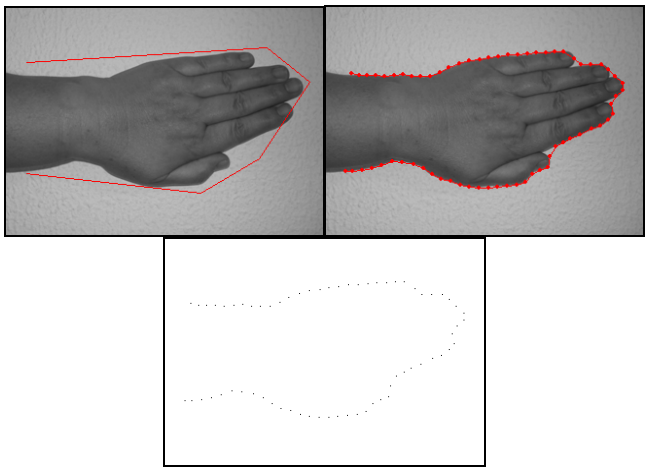

Figure 9: Initial contour (top left); result of the segmentation with r=2,000N/m considering a model with 66 nodes and made of rubber (top right); nodes of the contour extracted (bottom).

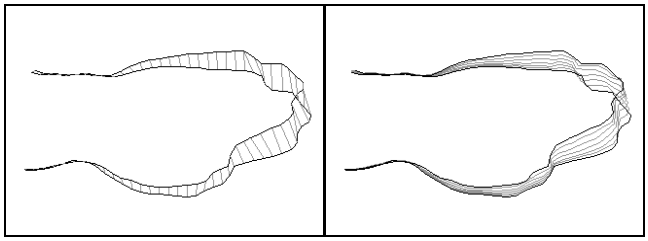

Figure 10: Matching between the two contours in Figs. 6 and 7 using global search (left); simulation obtained for the two contours (right – in black are the initial and target objects, and in grey five estimated shapes).

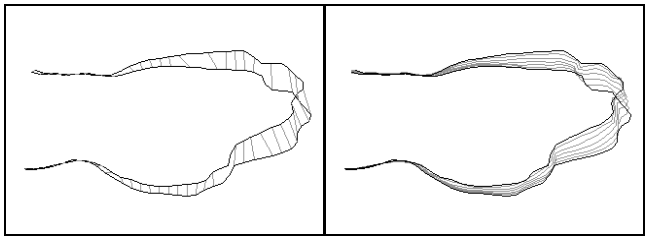

Figure 11: Matching between the two contours in Figs. 6 and 7 using local search (left); simulation obtained for the two contours (right – in black are the initial and target objects, and in grey five estimated shapes).

To overtake these drawbacks, in the near future some changes to fasten and improve the segmentation process will be introduced, such as trying different approaches for the definition of the external forces. The use of finite elements more suitable for large and nonlinear deformations is also a subject to be addressed in the following stages of this work.

In this paper a physical approach to simulate the deformation of objects represented in images was also described, and a solution that enables the application of the used approach to objects that do not have all of their nodes successfully matched was proposed.

The experimental results obtained in the matching process and in the estimation of the involved deformation are coherent with the physically expected behaviour of the modelled objects, validating the used approach. Although the results are quite satisfactory, the computation process is not very fast. So, in the future, to solve the dynamic equilibrium equation faster, parallel implementations will be considered. Also, to determine the external forces in the unmatched nodes other approaches will be developed.

To improve the matching process, Oliveira and Tavares (2008) approach will be used, that considers the order of the nodes of the contours preventing crossed matches, thus improving the matching quality, and, additionally, the computation time decreases considerably [Tavares, Carvalho, Oliveira, Reis, Vasconcelos, Gonçalves, Pinho and Ma (2008)].

The tracking of objects along image sequences, using the methodology here proposed complemented with stochastic methods to estimate the involved motion, is also a task that will be addressed in the near future.

Acknowledgements The presented work was partially done in the scope of the research project "Segmentation, Tracking and Motion Analysis of Deformable (2D/3D) Objects Using Physical Principles", with reference POSC/EEA-SRI/55386/2004, financially supported by *FCT - Fundação para a Ciência e a Tecnologia* in Portugal.

References:

Bastos, M. L.; Tavares, J. M. R. S. (2006): Matching of Objects Nodal Points Improvement Using Optimization. *Inverse Probl. Sci. Eng.*, vol. 14, pp. 529-541.

Bathe, K.-J. (1996): *Finite Element Procedures*. New Jersey, USA: Prentice-Hall.

Carvalho, F. J.; Tavares, J. M. R. S. (2006) Two Methodologies for Iris Detection and Location in Face Images. *Proc. of the CompIMAGE - Computational Modelling of Objects Represented in Images: Fundamentals, Methods and Applications,* Coimbra, Portugal, 20-21 October.

Cook, R.; Malkus, D.; Plesha, M. (1989): *Concepts and Applications of Finite Element Analysis*. New York, USA: John Wiley and Sons.

Gonçalves, P. C. T.; Pinho, R. R.; Tavares, J. M. R. S. (2006) Physical Simulation Using FEM, Modal Analysis and the Dynamic Equilibrium Equation. *Proc. of the CompIMAGE - Computational Modelling of Objects Represented in Images: Fundamentals, Methods and Applications,* Coimbra, Portugal, 20-21 October, pp. 197-204.

Kass, M.; Witkin, A.; Terzopoulos, D. (1988): Snakes: Active Contour Models. *Int. J. Comput. Vis.*, vol. 1, pp. 321-331.

Ma, Z.; Tavares, J. M. R. S.; Jorge, R. N. (2008): Segmentation of Structures in Medical Images: Review and a New Computational Framework. *CMBBE 2008 - 8th International Symposium on Computer Methods in Biomechanics and Biomedical Engineering,* Porto, Portugal, 27 February - 1 March

Nastar, C. (1994): *Modèles Physiques Déformables et Modes Vibratoires pour l'Analyse du Mouvement Non-Rigide dans les Images Multidimensionnelles*. Thèse de Doctorat, École Nationale des Ponts et Chaussées, Champs-sur-Marne, France.

Oliveira, F. P. M.; Tavares, J. M. R. S. (2008): Algorithm of Dynamic Programming for Optimization of the Global Matching Between Two Contours Defined by Ordered Points. *CMES: Computer Modeling in Engineering & Sciences (in press)*.

Pentland, A.; Horowitz, B. (1991): Recovery of Nonrigid Motion and Structure. *IEEE Trans. Pattern Anal. Mach. Intell.*, vol. 13, pp. 730-742.

Pinho, R. R.; Tavares, J. M. R. S. (2004a): Dynamic Pedobarography Transitional Objects by Lagrange's Equation with FEM, Modal Matching and Optimization Techniques. *Lect. Notes Comput. Sc.*, vol. 3212, pp. 92-99.

Pinho, R. R.; Tavares, J. M. R. S. (2004b) Morphing of Image Represented Objects Using a Physical Methodology. *Proc. of the 2004 ACM Symposium on Applied Computing,* Nicosia, Cyprus, pp. 10-15.

Sclaroff, S. (1995): *Modal Matching: a Method for Describing, Comparing, and Manipulating Digital Signals*. PhD Thesis, Massachusetts Institute of Technology, Cambridge, USA.

Sclaroff, S.; Pentland, A. (1995): Modal Matching for Correspondence and Recognition. *IEEE Trans. Pattern Anal. Mach. Intell.*, vol. 17, pp. 545-561.

Sethian, J. A. (1999): *Level Set Methods and Fast Marching Methods: Evolving Interfaces in Computational Geometry, Fluid Mechanics, Computer Vision, and Materials Science*. New York, USA: Cambridge University Press.

Shapiro, L. S.; Brady, J. M. (1992): Feature-based correspondence: an eigenvector approach. *Image Vision Comput.*, vol. 10, pp. 283-288.

Shen, J.; Castan, S. (1992): An Optimal Linear Operator for Step Edge Detection. *CVGIP: Graph. Models Image Process.*, vol. 54, pp. 112-133.

Sonka, M.; Hlavac, V.; Boyle, R. (2008): *Image Processing, Analysis, and Machine Vision*. USA: Thomson.

Tavares, J. M. R. S.; Barbosa, J.; Padilha, A. J. (2000) Matching Image Objects in Dynamic Pedobarography. *Proc. of the RecPad 2000 - 11th Portuguese Conference on Pattern Recognition,* Porto, Portugal, 11-12 May.

Tavares, J. M. R. S.; Carvalho, F. J. S.; Oliveira, F. P. M.; Reis, I. M. S.; Vasconcelos, M. J. M.; Gonçalves, P. C. T.; Pinho, R. R.; Ma, Z. (2008): Computer Analysis of Objects' Movement in Image Sequences: Methods and Applications. *Int. J. Comput. Vision Biomech (in press)*.

Terzopoulos, D.; Platt, J.; Barr, A.; Fleischer, K. (1987) Elastically deformable models. *Proc. of the 14th Annual Conference on Computer Graphics and Interactive Techniques,* Anaheim, USA, pp. 205-214.

Terzopoulos, D.; Witkin, A.; Kass, M. (1988): Constraints on Deformable Models: Recovering 3D Shape and Nonrigid Motion. *Artif. Intel.*, vol. 36, pp. 91-123.

Vasconcelos, M. J.; Tavares, J. M. R. S. (2006) Methodologies to Build Automatic Point Distribution Models for Faces Represented in Images. *Proc. of the CompIMAGE - Computational Modelling of Objects Represented in Images: Fundamentals, Methods and Applications,* Coimbra, Portugal, 20-21 October, pp. 435-440.

Wang, S. Y.; Lim, K. M.; Khoo, B. C.; Wang, M. Y. (2007a): A Geometric Deformation Constrained Level Set Method for Structural Shape and Topology Optimization. *CMES: Computer Modeling in Engineering & Sciences*, vol. 18, pp. 155-181.

Wang, S. Y.; Lim, K. M.; Khoo, B. C.; Wang, M. Y. (2007b): On Hole Nucleation in Topology Optimization Using the Level Set Methods. *CMES: Computer Modeling in Engineering & Sciences*, vol. 21, pp. 219-237.

Wang, S. Y.; Lim, K. M.; Khoo, B. C.; Wang, M. Y. (2007c): An Unconditionally Time-Stable Level Set Method and Its Application to Shape and Topology Optimization. *CMES: Computer Modeling in Engineering & Sciences*, vol. 21, pp. 1-40.

Wang, S. Y.; Wang, M. Y. (2006): Structural Shape and Topology Optimization Using an Implicit Free Boundary ParametrizationMethod. *CMES: Computer Modeling in Engineering & Sciences*, vol. 13, pp. 119-147.